# Dynamic Simulation of the Stability of Annular Flows in Gas Wells

## Amieibibama Joseph [a*] and Raphael Afolabi Peters [a]

[a] *Department of Petroleum & Gas Engineering, University of Port Harcourt, Nigeria.*

***Authors' contributions***

*This work was carried out in collaboration between both authors. Both authors read and approved the final manuscript.*

*Original Research Article*

## ABSTRACT

This paper provides a holistic view of the development and progression of multiphase gas-liquid annular flow in gas wells. With the help of a momentum balance, the stability of a fully developed annular flow is defined. The Euler-Euler model was used to model the multiphase flow system, while the Reynolds-Averaged Navier–Stokes (RANS) model was used to depict a time-dependent solution for a vertical fluid flow system, considering acceleration due to gravity and fluid compressibility. The resultant flow regime was tested for stability by gradually reducing the field velocity of flow and observing the effects using a computational fluid dynamics (CFD) software. The principal parameters considered are the superficial gas velocity and liquid film flow rate. The properties of the region where the flow becomes unstable are documented and related to the incidence of liquid loading in a typical gas well. The effect are critically observed and compared to flow regimes at lower superficial gas velocity. The resultant flow regime configurations are analyzed and compared to the annular flow system. This study will help researchers understand the behaviour of gas wells that have potential in developing liquid loading problems and the movement of liquid film on the wall of the tubing when in annular flow regime.

_____

*Corresponding author: E-mail: josephamiebibama @uniport.edu.ng;*

## NOMENCLATURE

$\rho_i$ = *density of phase i*

$\vec{V_i}$ = *velocity of phase i;*

$\dot{m}_{ji}$ = *mass transfer from phase j to phase i;*

$\dot{m}_{ij}$ = *mass transfer from phase i to phase j;*

$S_i$ = *source term;*

$\alpha_i$ = *volume fraction phase i;*

$\vec{F_i}$ = *external body force;*

$\vec{F}_{lift,i}$ = *lift force;*

$\vec{F}_{wl,i}$ = *wall lubrication force;*

$\vec{F}_{vw,i}$ = *virtual mass force;*

$\vec{F}_{td,i}$ = *turbulent dispersion force;*

$\vec{R}_{ji}$ = *interaction between phases;*

$p$ = *pressure shared by all the phases;*

$\vec{V}_{ji}$ *and* $\vec{V}_{ij}$ *represent the interphase velocities*

$U_i$ = *the mean velocity,*

$u_i'$ *is the fluctuating velocity components,*

$P_i$ *is the pressure gradient;*

*μ and ρ are the dynamic viscosity and density of the fluid;*

$\rho\overline{u_i'u_j'}$ *is the Reynolds stress tensor which represents the effects of the turbulence and is referred to as the Reynolds stress tensor,*

$G_k$ = *turbulence kinetic energy generation term;*

$G_b$ *is turbulence kinetic energy generation;*

$Y_m$ *is the contribution of the fluctuating dilatation in compressible turbulence to the overall dissipation rate;*

$C_{1\varepsilon}$, $C_{2\varepsilon}$ *and* $C_{3\varepsilon}$ *are constants;*

$\sigma_k$ *and* $\sigma_\varepsilon$ *are the turbulent Prandtl numbers for k and ε.*

$S_k$ *and* $S_\varepsilon$ *are user-defined source terms.*

$V_{sl}$ = *superficial liquid velocity*

$V_{sg}$ = *superficial gas velocity*

## 1. INTRODUCTION

At the initial stage of gas well production, entrained liquid is carried along the production tubing to the surface by the gas. As the well ages, gas velocity drops, and entrained liquid tends to fall back into the wellbore, thereby loading liquid at the wellbore and the gas flow will approach laminar flow [1]. According to Skopich et al. [2], unpredictable gas production and decreased produced liquid are caused by liquid loading. Gas wells mostly experience annular flow during their lifespan [3]. The transition of the annular flow regime to other flow regimes is usually gradual [4]. The consequence of a sudden change in the flow regime, especially when the gas velocity drops, is usually negative, thus problems such as liquid loading and flow reliability at the well head may be some of the major issues encountered when a sudden transition in flow regime occurs [5]. Liquid loading usually occurs when the natural energy (reservoir pressure) of the well is insufficient to guarantee the evacuation of produced liquids from the wellbore to the surface. Similarly, flow reliability is usually not guaranteed when there is a sudden disturbance or change in flow parameters of the well. For example, a sudden transition into slug flow may result in erratic deliverability of the wel [6]. Though these problems are planned for in the well development program, it is imperative to predict the probable time of these events using established models to analyze the flow pattern of the well. As noted by Adaze et al. [1], the interfacial structure and droplet entrainment mechanisms make the modelling of annular flow complex, and no exact analytical solution exists. Jayanti and Hewitt [7], analyzed a typical liquid

film flow in annular flow by fixed liquid film configuration. The film configuration was obtained directly from experimental observation. The analysis was subjected to both inlet and outlet boundaries at the interface, and it was observed that laminar flow exists in the liquid sub-layer.

There are curative and preventive methods that have been developed in managing liquid loading. Common curative methods include artificial lift methods to lift the accumulated liquids [8,9,10] while the preventive method employs predictive models to monitor its occurrence [11]. Although several models have been developed to predict liquid loading, none has the capability of accurately predicting its occurrence. The most viable ones considered modelling annular flow patterns to predict liquid loading and justify well interventions before the problem arises. Due to the uniqueness of wells around the world, it is imperative to properly identify the point at which the problem develops and propose a generalized model based on observed peculiarities.

To properly establish the stability of annular flows, the components of a typical annular flow must be studied. A typical annular flow in a conduit must consist of a core of gas with dispersed tiny liquid droplets and a thin film of liquid at the periphery. The film thickness, film velocity and pressure gradient of the regime have a triangular relationship [12]. This implies that evaluation of one of the parameters is easier if the other two are known. Skopich et al. [2] experimentally investigated the impact of pipe internal diameter on liquid hold-up using critical gas flow rate a in two-phase flow system.

Turner et al [13] extensively carried out studies on the annular core in relation to the minimum velocity that guarantees the evacuation of liquid from a gas well and reported the first attempt to predict the onset of liquid loading. Coleman et al [14] did same but at reservoir pressures lesser than 500 psi. Under this condition, the annular flow may start to behave in an erratic fashion as the gas velocity will be lower than that for higher reservoir pressures. Similarly, other researchers focused on the film thickness, flowrate and direction to support the behavior of annular flow. Luo et al. [15] showed that the variation observed in the liquid film may serve as an additional factor in understanding the stability of annular flow.

The film thickness of annular flow in a liquid-gas multiphase system is not exactly uniform across the entire section [16]. For ease of representation, a fully developed annular flow can be assumed to have a fairly uniform film thickness which is necessarily an average of the film thicknesses at each point in the wave surface [17]. Since, the gas flow rate and pressure gradient across the section inadvertently determine the movement of the film, this study aims to generate predictive equations for the relationship between the superficial gas flow rate and the film flow rate at varying superficial liquid velocities. Due to the paucity of data for this study, it is imperative to use a Computational Fluid Dynamic (CFD) software to simulate the multiphase flow dynamics for annular flow by inputting actual well conditions into an already established annular flow model. This provides instantaneous values of the minimum film velocity as the parameters are evaluated.

In this study, the conditions for the stability of annular flow in vertical gas wells was investigated using computational Fluid Dynamics software to give insight into the accumulation of liquids in the wellbore. This was achieved by simulating the annular flow pattern in a typical gas well and changing the boundary conditions to observe the resultant effect. This study will help researchers understand the behaviour of gas wells that have potential in developing liquid loading problems and the movement of liquid film on the wall of the tubing when in annular flow regime

## 2. METHODOLOGY

### 2.1 Simulating of Annular Flow

Owing to the multivariate nature of annular flow, the Euler-Euler model was used to model the multiphase flow system and the Reynolds-Averaged Navier–Stokes (RANS) model was used to model the turbulent flow system.

The Euler-Euler model is characterized by a two-phase (or multiphase) mixture having a continuous phase and a dispersed phase, similar to a typical fully developed annular flow where the gas is the continuous phase and the liquid is the dispersed phase. The Eulerian (Euler-Euler) multiphase model is widely used in multiphase flow system and is capable of modelling gas-liquid phase system [1], through independent conservation of mass and momentum equations (Equations 1 and 2)

Conservation of mass:

$$\frac{\partial}{\partial t}(\alpha_i \rho_j) + \nabla . \left(\alpha_i \rho_i \vec{V_i}\right) = \sum_{p=1}^{n}\left(\dot{m}_{ji} - \dot{m}_{ij}\right) + S_i \tag{1}$$

Conservation of momentum:

$$\frac{\partial}{\partial t}(\alpha_i \rho_i) + \nabla . \left(\alpha_i \rho_i \vec{V_i}\vec{V_i}\right) = \alpha_i \nabla j + \nabla . \overline{\overline{\tau}}_i + \alpha_i \rho_i \vec{g} + \sum_{p=1}^{n}\left(\vec{R}_{ji} + \dot{m}_{ji}\vec{V}_{ji} - \dot{m}_{ij}\vec{V}_{ij}\right) + \left(\vec{F}_i + \vec{F}_{lift,i} + \vec{F}_{wl,i} + \vec{F}_{vw,i} + \vec{F}_{td,i}\right) \tag{2}$$

Where $\rho_i$ is the density of phase I, $\vec{V_i}$ is the velocity of phase i; $\dot{m}_{ji}$ is the mass transfer from phase j to phase i; $\dot{m}_{ij}$ is the mass transfer from phase i to phase j; $S_i$ is a source term; $\alpha_i$ is the volume fraction of phase i; $\vec{F}_i$ is an external body force; $\vec{F}_{lift,i}$ is a lift force; $\vec{F}_{wl,i}$ is a wall lubrication force; $\vec{F}_{vw,i}$ is a virtual mass force; $\vec{F}_{td,i}$ is a turbulent dispersion force; $\vec{R}_{ji}$ is an interaction between phases; p is the pressure shared by all the phases; $\vec{V}_{ji}$ and $\vec{V}_{ij}$ represent the interphase velocities defined in Equations 3 and 4.

$$\text{for } \dot{m}_{ji} > 0, \qquad \vec{V}_{ji} = \vec{V_j}, \quad \text{for } \dot{m}_{ji} < 0, \qquad \vec{V}_{ji} = \vec{V_i} \tag{3}$$

$$\text{for } \dot{m}_{ij} > 0, \qquad \vec{V}_{ij} = \vec{V_i}, \quad \text{for } \dot{m}_{ij} < 0, \qquad \vec{V}_{ij} = \vec{V_j} \tag{4}$$

$\overline{\overline{\tau}}_q$ is the stress-strain tensor in phase i, given as:

$$\overline{\overline{\tau}}_i = \alpha_i \mu_i \left(\nabla \vec{V_i} + \nabla \vec{V_i}^T\right) + \alpha_i \left(\lambda_i - \frac{2}{3}\mu_i\right)\nabla . \vec{V_i}\overline{\overline{I}} \tag{5}$$

$\alpha_i$ is the shear viscosity of phase i; $\lambda_i$ is the bulk viscosity of phase i.

The above model uses the Navier-Stokes equations to solve for the velocity field. The resultant velocity was then compared with the momentum balance expression.

Reynolds number defines the type of flow, whether laminar or turbulent. The Reynolds number in this study indicates that flow is turbulent even though the fluid assumes a streamlined formation. Similarly, the liquid film is believed to have a laminar flow form [18], while the gas core may be 'laminarized' by the degree of entrainment of liquid in the gas phase [12].

A typical multiphase system flowing in the annular region may be conditioned to operate under the Reynolds-Averaged Navier–Stokes (RANS) model. Equations 6 and 7 are the Cartesian coordinates of the RANS continuity for mass and momentum equations for the flow.

Continuity equation:

$$\frac{\partial P}{\partial t} + \frac{\partial}{\partial x_i}(\rho U_i) = 0 \tag{6}$$

Momentum equation:

$$\frac{\partial}{\partial t}(\rho U_i) + \frac{\partial}{\partial x_j}\left(\rho U_i U_j\right) = -P_i + \frac{\partial}{\partial x_j}\left(\mu\left(\frac{\partial U_i}{\partial x_j} + \frac{\partial U_j}{\partial x_i}\right)\right) - \frac{\partial}{\partial x_j}\left(\rho\overline{u_i'u_j'}\right) \tag{7}$$

$$\rho\overline{u_i'u_j'} = u_t\left(\frac{\partial U_i}{\partial x_j} + \frac{\partial U_j}{\partial x_i}\right) - \frac{2}{3}\rho\delta_{ij}k \tag{8}$$

where;
k is the turbulent kinetic energy, given as:

$$k = \frac{1}{2}\overline{u_i'u_j'} \tag{9}$$

and $u_t$ is the turbulent Eddy viscosity which is a function of $k$ and $\varepsilon$ turbulent model. The $k - \varepsilon$ model is defined in Equation 10 and 11.

$$\frac{\partial}{\partial t}(\rho k) + \frac{\partial}{\partial x_i}(\rho U_i k) = \frac{\partial}{\partial x_j}\left(\left(\mu + \frac{\mu_t}{\sigma_k}\right)\frac{\partial k}{\partial x_j}\right) + G_k + G_b - \rho\varepsilon - Y_m + S_k \qquad (10)$$

And

$$\frac{\partial}{\partial t}(\rho\varepsilon) + \frac{\partial}{\partial x_i}(\rho U_i \varepsilon) = \frac{\partial}{\partial x_j}\left(\left(\mu + \frac{\mu_t}{\sigma_\varepsilon}\right)\frac{\partial\varepsilon}{\partial x_j}\right) + C_{1\varepsilon}(G_k + C_{3\varepsilon}G_b) + C_{2\varepsilon}\rho\frac{\varepsilon^2}{k} + S_\varepsilon \qquad (11)$$

where $G_k$ is the turbulence kinetic energy generation term; $G_b$ is the turbulence kinetic energy generation; $Y_m$ is the contribution of the fluctuating dilatation in compressible turbulence to the overall dissipation rate; $C_{1\varepsilon}$, $C_{2\varepsilon}$ and $C_{3\varepsilon}$ are constants; $\sigma_k$ and $\sigma_\varepsilon$ are the turbulent Prandtl numbers for $k$ and $\varepsilon$, respectively. The $S_k$ and $S_\varepsilon$ are user-defined source terms. In the $k$ and $\varepsilon$ model, the turbulent viscosity is calculated from Equation 12:

$$\mu_t = \rho C_\mu \frac{k^2}{\varepsilon} \qquad (12)$$

where $C_\mu$ is a constant.

The k-ε model suites the annular flow model and the only assumption is that the flow is anisotropic for the entire length of the well. The aim of utilizing the CFD software is usually to solve the Partial Differential Equations (PDEs) of the flow's multivariate function. The major task is to control the properties of the fluids in a user-defined environment to match the selected flow and geometry.

It is imperative to define the boundary conditions to constrain the probable solutions of the flow function. The definition of the geometry, fluid characteristics, inlet and outlet conditions should resemble real life situations as best possible. The focus will be on defining the necessary parameters and allowing the interacting fluid to conform the geometry based on the RANS model. The typical features of the annular flow are evident; and the liquid section of the flow will form a thin film on the periphery of the pipe [4], while there is a core containing tiny dispersed molecules of liquid in the gas phase as a result of the strong turbulence energy of the flow.

## 2.2 Geometry of Flow

The flow is represented in a 2-dimensional configuration to restrict the number of iterations and the degree of freedom of the resultant PDEs. It constitutes one rectangle with a dimension of 2" x 3", and 10 rectangles with dimensions of 0.05" x 0.1". The hypothetical orientation of the geometry is shown in Fig. 1.
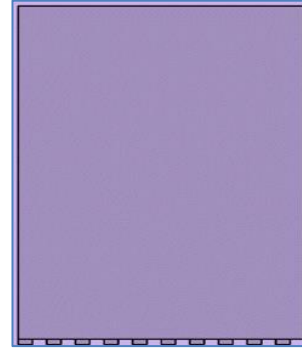


**Fig. 1. 2D Rectangular dimensions**

## 2.3 Selection

Methane gas and transformer oil were selected as the fluids since their average properties are similar to those typical found in a gas well. Due to the phase concentration of the gas relative to the liquid in this flow pattern, the compressibility of the fluid is considered as the Mach number is less than 0.3. The most sensitive property in this case is the density, which is defined by the software for each fluid species. Additionally, it is assumed that there is no evident chemical reaction between the fluids.

### 2.3.1 Inlet conditions for gas and liquid:

a) Instead of a normal inflow velocity, a velocity field is selected with direction restricted to the y-axis. It is assumed that there is no x-axis movement of gas at the inlet condition.

b) The field velocity was selected to increase progressively as follows: 0.1m/s, 0.5m/s, 1m/s, 2m/s, 3m/s, 4m/s, 5m/s, and 6m/s respectively.
c) The differential equation form of the CFD is solved using the discretization model of the interacting fluids.
d) Normal inflow velocity is used for the liquid component and the velocity is fixed at 0.01m/s, 0.05m/s and 0.1m/s for all the varying inlet gas conditions.
e) The density of the liquid is assumed constant based on the temperature of reference. Although, the density may vary slightly as the temperature in the well changes and at different mixing conditions with the gas in the annular model

## 2.4 Wellbore Conditions

The condition of any well is not static; however, to properly display the annular flow pattern and possible instance of liquid loading, certain conditions have been set for temperature and pressure.

It was assumed that the bottomhole flowing pressure is 5MPa while the temperature range is 353.15 - 373.15K. These values were keyed into the input point of the geometry's space domain to cover the entire flowing area of the gas and liquid interacting in the well.

### 2.4.1 Liquid and gas domain

In order to establish the annular flow model in the software, the liquid and gas must have unique domains at $t = 0 \, sec$. These domain evolve as the steady state fluid flow progresses. The domains are shown in Fig. 2. The selection is typical of the nature of annular flows. The gas

domain occupies a larger percentage of the geometry than the liquid domain. Overall, the choice is made based on the nature of the flow regime. The phase fraction of the gas in annular flow is always greater than that of the liquid since the gas is the continuous phase; this is characteristic of 2-phase annular flows.

### 2.4.2 Theory of stability

The theory of stability of the annular flow relies on the momentum balance of the interacting fluids, with the film reversal theory also being a factor. At high gas velocities, a full profile of the annular flow is developed as shown in Fig. 3. To establish a stable 2-phase annular flow, there must be a steady state flow with a defined gas core and liquid film on the conduit walls.

The point of liquid loading, assumed to be the point where a typical annular flow becomes unstable, will be the point by examining the momentum balance of the interacting fluid. The effect of this can be properly understood by comparing the velocity of the gas stream with the velocity of the liquid film. The destabilization of the annular flow can then be studied in-depth since the momentum balance is based on the reversal theory.

## 2.5 Mesh Selection and Justification

The mesh used is the free triangle model which consists of a total of 653 triangles for the considered geometry (Table 1 and Fig. 4). The selection, though considered an extremely coarse framework, makes the solution quicker to solve. A fine framework was also selected and the time step solution graph was similar with very minute errors. The total degree of freedom (DOF) solved for in the time dependent solution is 4869 which includes 2613 internal DOFs.
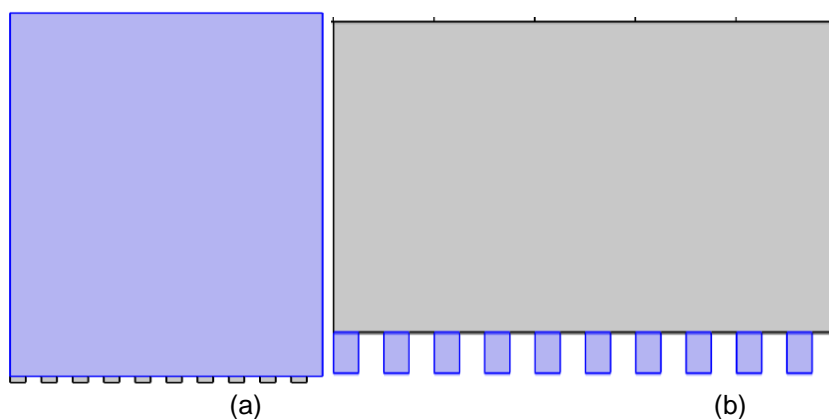


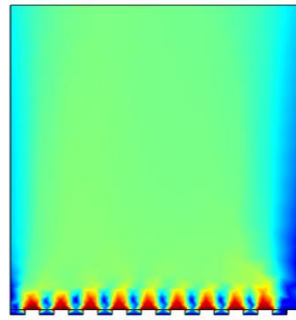**Fig. 2. 2D Fluid Domain (a) gas-methane and (b) liquid- Transformer Oil**

**Fig. 3. 2D Annular Flow Development in a 2-Phase System**

**Table 1. Mesh Data**

| Description | Values |
| --- | --- |
| Minimum Element Quality | 0.7514 |
| Average Element Quality | 0.9445 |
| Number of Triangle | 653 |
| Number of Edge Element | 117 |
| Number of Vertex Element | 43 |
| Calibrated for | Fluid Mechanics |
| Maximum Element Size | 0.26 |
| Minimum Element Size | 0.01 |
| Curvature Factor | 0.8 |
| Maximum Element Growth Rate | 1.3 |
| Predefined Size | Extremely Coarse (Selected to ease calculation) |
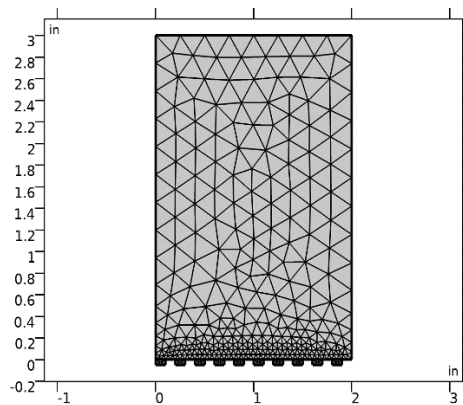


**Fig. 4. 2D Triangular mesh framework of the annular flow system**

## 3. RESULTS AND DISCUSSION

### 3.1 Relationship between Gas Velocity and Minimum film Thickness Velocity

The velocity of the liquid film is of great significance because it is an offshoot of the superficial gas velocity. Fig. 5 shows the relationship between gas velocity and minimum film velocity for $V_{sl}$ of 0.01 m/s. The curve shows a polynomial relationship between the two parameters in the annular flow regime. As the gas velocity increases, it reaches a point where the minimum film velocity remains constant. This

can be observed to occur at $V_{sg} = 4 \, \text{m/sec}$ and beyond. Another critical point in this curve is the lowest point, which occurs at $V_{sg} = 0.5 \, \text{m/sec}$ with an equivalent minimum film velocity of 0.000228m/s. This appears strange because at a much lower $V_{sg} = 0.1 \, \text{m/sec}$, the minimum film velocity is 0.000583m/s. The phenomenon is better explained by considering a frame-by-frame solution of the computational fluid dynamics for elemental increases in parameters. It is evident that at very low $V_{sg}$ and $V_{sl}$, accurately determining the exact minimum film velocity is challenging. On the contrary, at high gas velocity,

7

the velocity of the film appears stable and defined.

For $V_{sl} = 0.01\,\mathrm{m/s}$, Fig. 5 was fitted with a polynomial of degree 4 with a best fit of 0.9937. However, for $V_{sl} = 0.05\,\mathrm{m/sec}$, Fig. 6, which exhibits similar curve, was fitted with a polynomial of degree 5 with a best fit of 0.9988. At increasing $V_{sg}$, the minimum film velocity stabilizes (beyond $V_{sl} = 6\,\mathrm{m/sec}$). The lowest point in the curve also depicts the uncertainty of estimating parameters at low $V_{sg}$ and $V_{sl}$ in an annular flow system.

For Fig. 7 which has a higher $V_{sl}$ compared to Figs. 5 and 6, a similar trend was observed but with a polynomial of degree 6 with a best fit of 0.9995. Cumulatively, the observed trend depicts an important relationship existing between gas velocity and liquid film velocity in an annular flow system.

Sustaining an annular flow regime in a multiphase domain is important for the deliverability of a gas well. However, this cannot be guaranteed at low well pressures and velocity. The domain of instability of a multiphase annular flow is very broad because several factors contribute to this. To properly establish this fact, a simple simulation of multiphase annular flow is established by imposing a disturbance into the matrix of an already developing flow. This disturbance will take different forms and the effect is expressed by the last recorded time step for time dependent solution of the PDEs whether they converge or not.
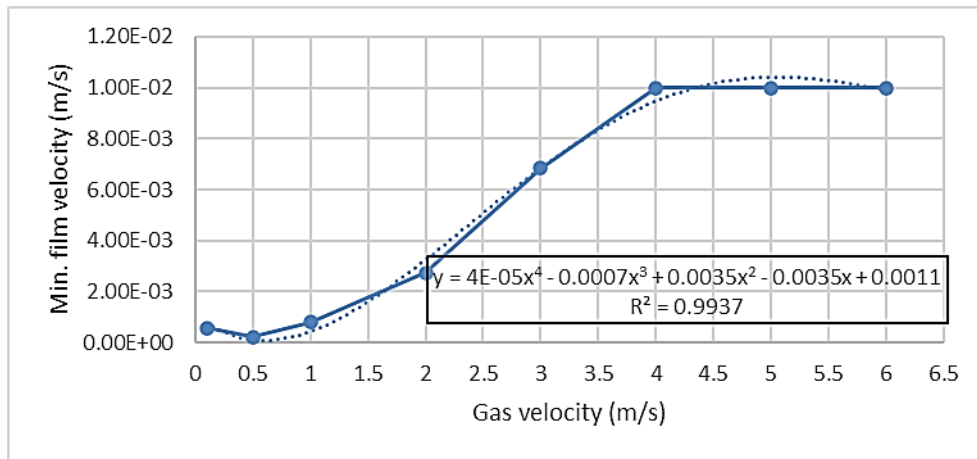


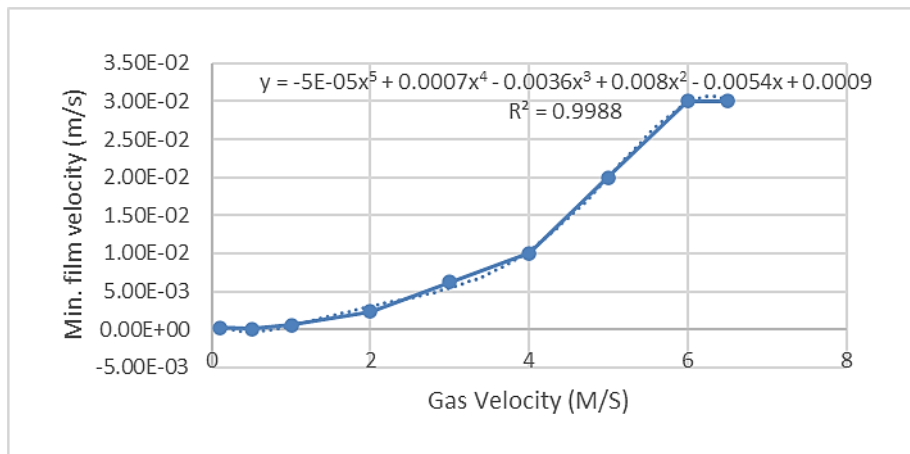**Fig. 5. Relationship between minimum film velocity and superficial gas velocity at Vsl = 0.01m/s**



**Fig. 6. Relationship between minimum film velocity and superficial gas velocity at $V_{sl} = 0.05$m/s**
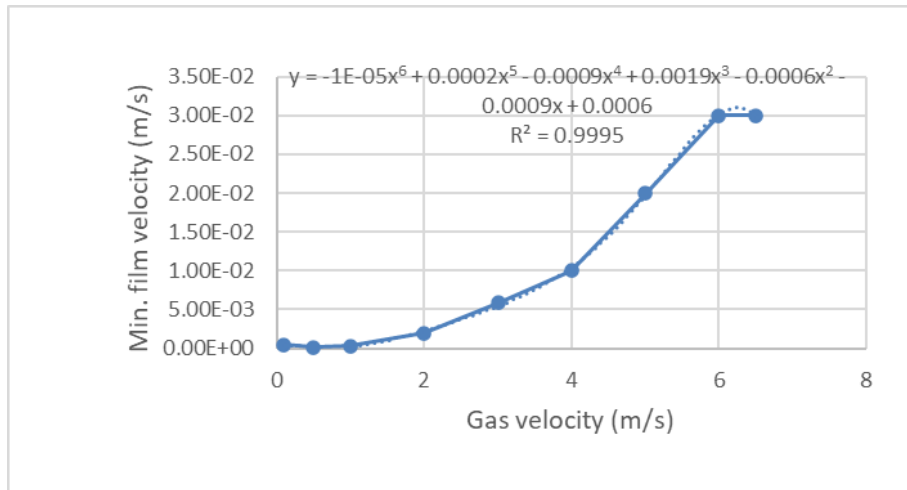
**Fig. 7. Relationship between minimum film velocity and superficial gas velocity
at $V_{sl} = 0.05$ m/s**

## 3.2 Incursion of Liquid into a Developing Annular Multiphase Flow

A sudden increase in liquid inflow into a developing annular system can disrupt the nature of the flow regime. This was achieved by increasing the contribution of the liquid phase by as low as 0.1% for initial conditions of $V_{sl} = 0.05$ m/s and $V_{sl} = 3$ m/s. The resultant effect is shown in Fig. 8b. Comparing it to Fig. 8a with the exact same initial condition but with only the stated variations, significant disparities can be noted. Most importantly, the direction of the resultant movement of particles in Fig. 8a

suggest that the gas well is producing against the acceleration due to gravity, indicated by the red arrows pointing upwards to show the direction of flow. On the contrary, Fig. 8b shows that there is indeed no production in the gas well and the annular multiphase flow sequence has been destroyed. No liquid film is observed and the flow is difficult to characterize. Furthermore, the developing annular flow shows that the time dependent solution converged at the input time of $t = 1$ second, while the other shows $t = 0.0032866$ second, confirming the solution was inconclusive and did not converge.
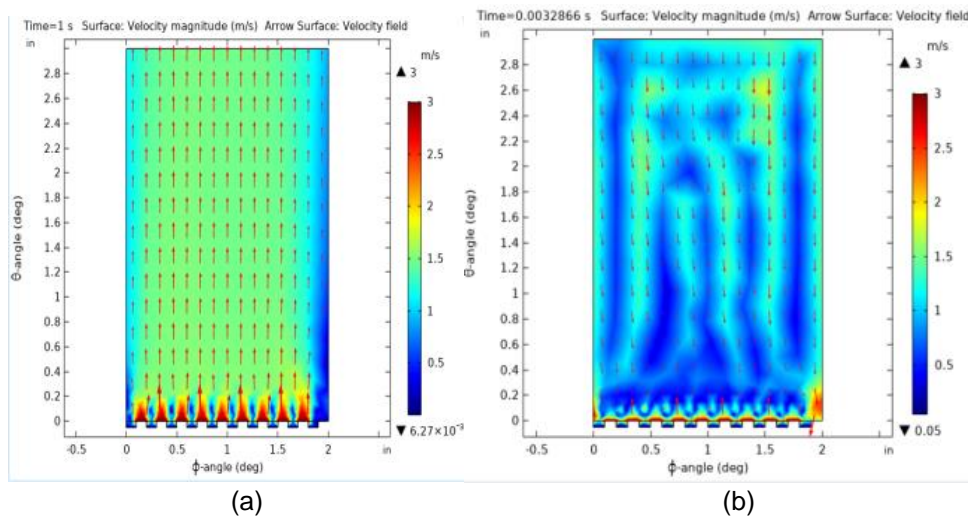


(a)  (b)

**Fig. 8. Simulation of annular flow regime at varying initial inlet conditions**
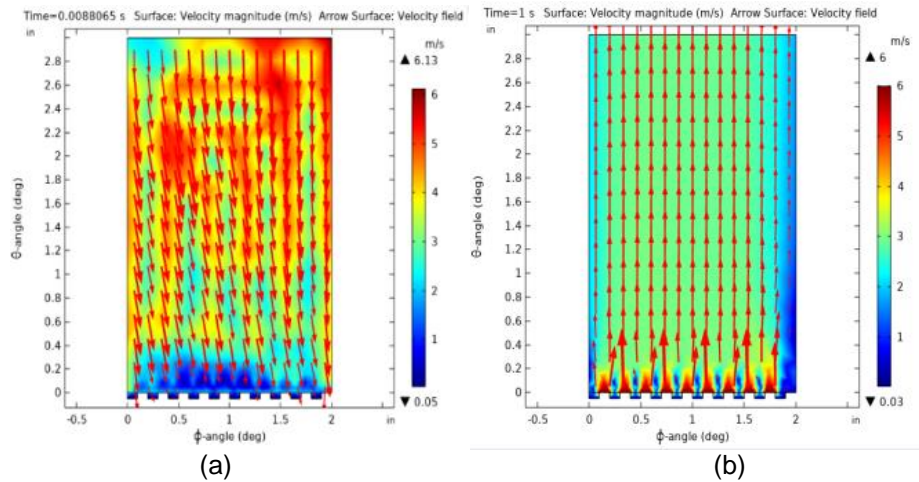
**Fig. 9. Simulation of annular flow regime at a drop in Velocity of the Gas**

## 3.3 Sudden Drop in Superficial Gas Velocity

The dual-phase annular flow continues to exist as long as no parameter is altered in the system. If the superficial gas velocity were to be reduced abruptly as against gradually, the disturbance in the system leads to accumulation of liquid in the wellbore. This is shown in Fig. 9a. At the upper portion of this diagram, it is clear that the gas velocity was sufficiently high to sustain the annular flow, especially when compared to Fig. 9b. However, a sudden drop in the superficial gas velocity results in the accumulation of liquid close to the inlet of the annular system, thereby impeding gas flow. Similarly, the flow direction arrow shows the downward movement of fluid in the system when compared to a flow at constant superficial gas velocity.

## 4. CONCLUSION

A dynamic simulation is developed to study the stability of multiphase annular flow in a gas well. A new consideration to include the minimum film velocity as an important parameter in this study was established. The study focussed on the components of a developed multiphase annular flow with a particular attention to the quality of the film. A destruction of the liquid film profile inadvertently destroys the annular flow regime. Certain factors may be attributed to the disruption of this profile. These factors were itemized with the help of a computational fluid dynamic simulation of the flow regime at varying boundary conditions. The actual setup of the model put into account the Reynolds-Averaged Navier–Stokes (RANS) model with $\text{Mach Number} > 0.3$, confirming a compressible

flow due to the gas component of the multiphase flow. The results of the simulation are observed to buttress the following conclusions:

i. The stability of a vertical/inclined multiphase annular flow system is guaranteed when there is a gas core with dispersed liquid and a liquid film along the wall of the flow path moving in the same direction against the gravitational pull of the environment.

ii. The minimum film velocity provides better insight into the region of instability of a fully developed multiphase annular flow.

iii. The disruption of the annular profile can be achieved if there is a sudden variation in flow parameters that distorts the pressure profile of the flow system.

iv. Any occurrence that disrupts the stability of the annular flow at low pressure leads to a temporary or permanent liquid loading of the system.

## COMPETING INTERESTS

Authors have declared that no competing interests exist.

## REFERENCES

1. Adaze E, Al-Sarkhi A, Badr, HM, Elsaadawy E. Current status of CFD modeling of liquid loading phenomena in gas wells: a literature review. Journal of Petroleum Exploration and Production Technology. 2018;9:1397–1411
Available: https://doi.org/10.1007/s13202-018-0534-4.

2. Skopich A, Pereyra E, Sarica C, Kelkar M. Pipe-diameter effect on liquid loading in

vertical gas wells. SPE Production & Operations. 2015; 30(02): 164-176.

3. Veeken K, Hu B, Schiferli W. Gas-well liquid-loading-field-data analysis and multiphase-flow modeling. SPE Production & Operations. 2010; 25(03): 275-284.

4. Bruno TJ. Conditioning of flowing multiphase samples for chemical analysis. Separation Science and Technology. 2005; 40(8):1721-1732.

5. Guo B,Chapter 5 - Productivity of wells with simple trajectories, in Well Productivity Handbook (Second Edition), Gulf Professional Publishing, 2019,p. 123-161.
   Available: https://doi.org/10.1016/B978-0-12-818264-2.00005-1.

6. Zhuang H, Han Y, Sun H, Liu X. Chapter 3 - Gas well deliverability test and field examples, In Dynamic Well Testing in Petroleum Exploration and Development (Second Edition), Elsevier. 2020;85-195,
   Available: https://doi.org/10.1016/B978-0-12-819162-0.00003-4.

7. Jayanti S, Hewitt GF. Hydrodynamics and heat transfer in wavy annular gas–liquid low: a computational fluid dynamics study. International Journal of Heat Mass Transfer. 1997; 40(10):2445–2460.

8. Huang F, Veeken KCAM, Chapter 8 - Foam-assisted liquid lift, In Oil and Gas Chemistry Management Series, Flow Assurance, Gulf Professional Publishing, Volume 1, 2022,Pages 541-608.
   Available: https://doi.org/10.1016/B978-0-12-822010-8.00001-5

9. Han W, Lv H, Fan J, Qiang T, Liu C, Ji Y, Dong S. Investigation of a highly efficient foaming mixture compromising cationic Gemini-zwitterionic-anionic surfactants for gas well deliquification. Tenside Surfactants Detergents, 2024.
   Available: https://doi.org/10.1515/tsd-2023-2572

10. Johri N, Kadam S, Veeken K, Prakash A, Suvarna H, Singh P, Daukia S, Kadirus S, Goswami A, Aakash S. Conquer Liquid Loading in Raageshwari Gas Field by Automated Intermittent Production and Deliquification Paper presented at the ADIPEC, Abu Dhabi, UAE, October 2023. Paper Number: SPE-216233-MS
    Available: https://doi.org/10.2118/216233-MS

11. Belyadi H, Fathi E, Belyadi F, Chapter Twenty-Five - Numerical simulation of real field Marcellus shale reservoir development and stimulation, in Hydraulic Fracturing in Unconventional Reservoirs (Second Edition), Gulf Professional Publishing, 2019,p. 541-585,
    Available: https://doi.org/10.1016/B978-0-12-817665-8.00025-4.

12. Jensen MK. The liquid film and the core region velocity profiles in annular two-phase flow. International Journal of Multiphase Flow. 1987;13(5):615-628.

13. Turner RG., Hubbard MG, Dukler AE. Analysis and prediction of minimum flow rate for the continuous removal of liquids from gas wells. Journal of Petroleum Technology. 1969;21(11):1-475.

14. Coleman SB, Clay HB, McCurdy DG, Norris III, L. H. A new look at predicting gas-well load-up. Journal of Petroleum Technology. 1991;43(03):329-333.

15. Luo S, Kelkar M, Pereyra E. Sarica C. A new comprehensive model for predicting liquid loading in gas wells. SPE Production & Operations. 2014; 29(04): 337-349.

16. Wang R, Lee BA, Lee JS, Kim KY, Kim S. Analytical estimation of liquid film thickness in two-phase annular flow using electrical resistance measurement. Applied Mathematical Modelling. 2012;36(7):2833-2840.

17. Srivastava RPS. Liquid film thickness in annular flow. Chemical Engineering Science. 1973;28(3):819-824.

18. White FM, Corfield I. Viscous fluid flow, McGraw-Hill Higher Education, Boston. 2006;3.